

Supporting Information

Photothermal response and precise control of circularly polarized luminescence via double-layered films based on cholesteric liquid crystal

Sha Huang, Qimei Wu, Yongjie Hu, Xincan Wang, Yongjie Yuan,* and Hailiang Zhang*

Key Laboratory of Polymeric Materials and Application Technology of Hunan Province, Key Laboratory of Advanced Organic Functional Materials of Colleges and Universities of Hunan Province, College of Chemistry, Xiangtan University, Xiangtan 411105, Hunan Province, China.

* Corresponding author

E-mail: hailiangzhang@xtu.edu.cn; yuanyongjie@xtu.edu.cn

Materials

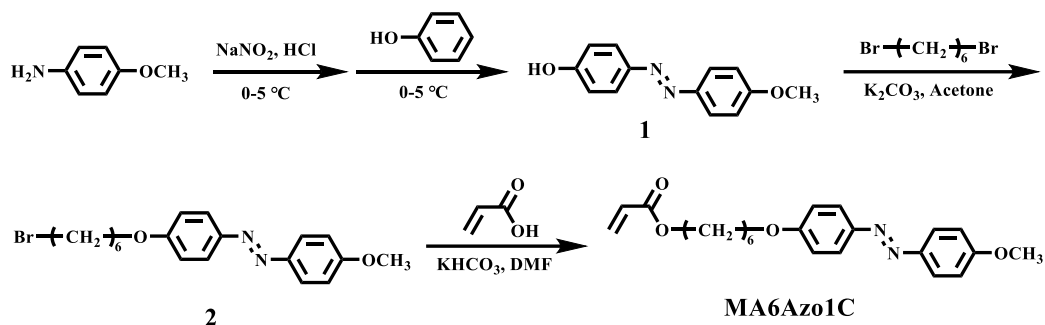
4-Methoxyaniline (99%), phenol (99%), 1,6-dibromohexane (98%), acrylic acid (99%), L-menthol (98%), methacryloyl chloride (97%), 4-bromo-1,8-naphthalic anhydride (98%), 4-aminophenol (99%), N,N-dimethyl-4-(4,4,5,5-tetramethyl-1,3,2-dioxaborolan-2-yl)aniline (98%), tetrakis(triphenylphosphine)palladium (99%), sodium nitrite (99%), sodium hydroxide (98%), potassium carbonate (99%), potassium iodide (99%), potassium bicarbonate (99%) and magnesium sulfate (99%) were purchased from Energy Chemical Company without further purification. Hydrochloric acid (AR), ethanol (AR), acetone (AR), petroleum ether (AR), N,N'-dimethylformamide (AR), methylene chloride (AR), triethylamine (AR) and tetrahydrofuran (AR) were purchased from Huihong Reagent

Co., Ltd. Among them, methylene chloride and tetrahydrofuran were refined by distilling to remove water. 2,2'-Azobis(2-methylpropionitrile) (AIBN, 98%) was purchased from Energy Chemical Company and was recrystallized in ethanol before use.

Measurements and Characterizations

The ^1H NMR and ^{13}C NMR spectra of all samples were measured by a Bruker ARX 400 MHz spectrometer. The molecular weight of intermediates and monomers were determined by Bruker Biflex III MALDI-TOF spectrometer and Agilent Technologies 1260 II/6230 LC/MS spectrometer. Waters 1515 GPC was employed to measure the number average molecular weight (M_n) and polydispersity index (PDI) of polymers. The thermal stability of samples was characterized by a TA Q50 instrument. The phase textures and their change of samples during the cooling process were characterized by a Leica DM 4500 P polarizing microscope instrument (POM). The phase transition temperature of samples was measured by a TA Q10 DSC instrument under N_2 atmosphere. The phase structure of samples was confirmed by a high-flux X-ray instrument (SAXSess mc², Anton Paar) equipped with a Kratky block collimation system and a GE ID3003 sealed-tube X-ray generator (Cu Ka). The UV-vis diffuse reflectance spectra were evaluated by ultraviolet-visible-near-infrared spectrophotometer (UH5700) with integrating sphere. The UV-vis absorption spectra of the samples were tested by Agilent Cary 100 instrument. The fluorescence spectra of samples were recorded on a PTI Qm 40 luminescence spectrometer. The circular dichroism (CD) spectra of samples were recorded on a JASCO J-1500 instrument, and a JASCO CPL-300 instrument was used to record CPL emission spectra. The photochemical isomerization of chiral liquid crystal films was studied by using 365 nm (600 mW cm^{-2}) FUWO UV-6BK UV LED.

Synthesis of monomers

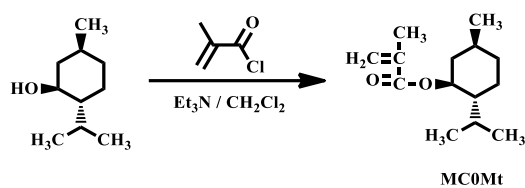


Scheme S1. The synthetic route of monomer MA6Azo1C.

Compound 1: ^1H NMR (400 MHz, δ , ppm, CDCl_3): 7.86 (dd, $J = 19.2, 8.8$ Hz, 4H, Ph-H); 6.92-7.01 (dd, $J = 30.0, 8.8$ Hz, 4H, Ph-H); 5.67 (s, 1H, -OH), 3.88 (s, 3H, -OCH₃).

Compound 2: ^1H NMR (400 MHz, δ , ppm, CDCl_3): 7.87 (dd, $J = 8.0, 4.4$ Hz, 4H, Ph-H); 6.99 (t, $J = 7.6$ Hz, 4H, Ph-H); 4.03 (t, $J = 6.4$ Hz, 2H, -CH₂-), 3.88 (s, 3H, -OCH₃), 3.67 (t, $J = 6.4$ Hz, 2H, -CH₂-), 1.56 (m, 8H, -CH₂-).

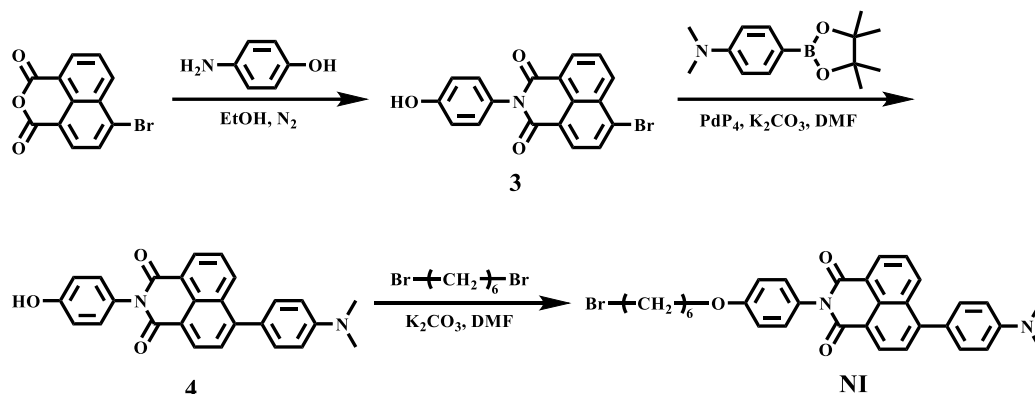
Monomer MA6Azo1C: ^1H NMR (400 MHz, δ , ppm, CDCl_3): 7.89 (dd, $J = 8.8, 4.0$ Hz, 4H, Ph-H); 6.99 (t, $J = 7.6$ Hz, 4H, Ph-H); 6.41 (dd, $J = 17.2, 1.2$ Hz, 1H, =CH₂); 6.13 (dd, $J = 17.6, 10.4$ Hz, 1H, =CH-); 5.82 (dd, $J = 10.4, 1.2$ Hz, 1H, =CH₂); 4.18 (t, $J = 6.4$ Hz, 2H, -CH₂-); 4.04 (t, $J = 6.4$ Hz, 2H, -CH₂-); 3.89 (s, 3H, -OCH₃); 1.84 (m, 2H, -CH₂-); 1.73 (m, 2H, -CH₂-); 1.52 (m, 4H, -CH₂-). ^{13}C NMR (100 MHz, δ , ppm, CDCl_3): 166.4, 161.6, 161.2, 147.0, 146.9, 130.6, 128.6, 124.4, 114.7, 114.2, 68.1, 64.5, 55.6, 29.1, 28.6, 25.8. Mass Spectrometry (MS) (m/z) [M]⁺ Calcd for C₂₂H₂₆N₂O₄, 382.19; found 382.30 [M]⁺.



Scheme S2. The synthetic route of monomer MC0Mt.

Monomer MC0Mt: ^1H NMR (400 MHz, δ , ppm, CDCl_3): 6.07 (s, 1H, =CH₂); 5.51 (s, 1H, =CH₂); 4.73 (td, $J = 12.0, 8.0$ Hz, 1H, -OCH-); 2.03 (m, 1H, -CH-); 1.93 (s, 3H, -CH₃); 1.86 (ddd, $J = 16.0, 4.0, 2.8$ Hz, 1H, -CH-); 1.68 (m, 2H, -CH₂-); 1.53 (m, 1H, -CH₂-); 1.42 (m, 1H, -CH₂-); 1.27 (m, 1H, -CH-); 0.88 (m, 8H, -CH₃); 0.76 (d, $J = 4.0$ Hz, 3H, -CH₃). ^{13}C NMR (100 MHz, δ , ppm, CDCl_3): 166.96, 136.85, 124.87, 74.40, 47.13, 40.84, 34.29, 31.37, 26.41, 23.56, 22.03, 20.74, 18.39, 16.45. Liquid Chromatograph Mass Spectrometry (LC-MS) (m/z) [M] Calcd for $\text{C}_{14}\text{H}_{24}\text{O}_2$, 224.18; found 247.17 [M+Na]⁺.

Synthesis of compound NI



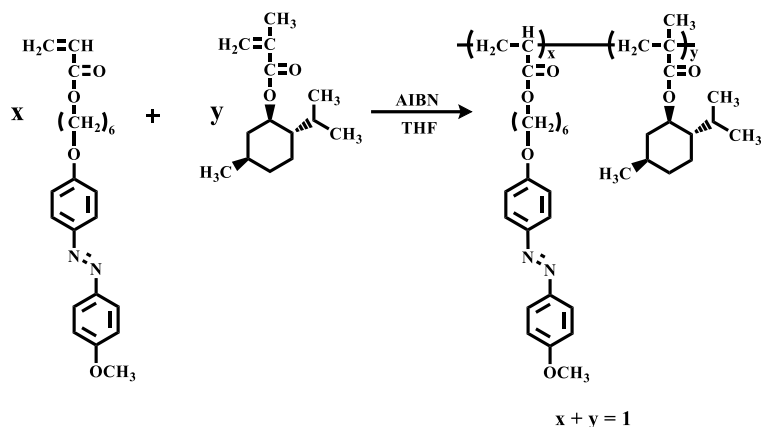
Scheme S3. The synthetic route of compound NI.

Compound 3: ¹H NMR (400 MHz, δ, ppm, DMSO-d₆): 9.72 (s, 1H, -OH); 8.46 (t, J = 7.6 Hz, 2H, Ph-H); 8.23 (d, J = 8.0 Hz, 1H, Ph-H); 8.13 (d, J = 8.0 Hz, 1H, Ph-H); 7.92 (t, J = 8.0 Hz, 1H, Ph-H); 7.13 (d, J = 8.8 Hz, 2H, Ph-H); 6.86 (d, J = 8.4 Hz, 2H, Ph-H).

Compound 4: ¹H NMR (400 MHz, δ, ppm, DMSO-d₆): 9.60 (s, 1H, -OH); 8.47 (t, J = 7.6 Hz, 2H, Ph-H); 8.39 (d, J = 8.4 Hz, 1H, Ph-H); 7.82 (t, J = 8.0 Hz, 1H, Ph-H); 7.73 (d, J = 7.6 Hz, 1H, Ph-H); 7.41 (d, J = 8.4 Hz, 2H, Ph-H); 7.11 (d, J = 8.4 Hz, 2H, Ph-H); 6.88 (dd, J = 20.8, 8.4 Hz, 4H, Ph-H); 2.99 (s, 6H, -CH₃).

Compound NI: ¹H NMR (400 MHz, δ, ppm, CDCl₃): 8.66 (m, 2H, Ph-H); 8.48 (d, J = 8.4 Hz, 1H, Ph-H); 7.71 (t, J = 6.0 Hz, 2H, Ph-H); 7.46 (d, J = 8.8 Hz, 2H, Ph-H); 7.24 (d, J = 8.8 Hz, 2H, Ph-H); 7.06 (d, J = 8.8 Hz, 2H, Ph-H); 6.90 (d, J = 8.4 Hz, 2H, Ph-H); 4.03 (t, J = 6.4 Hz, 2H, -CH₂-); 3.45 (t, J = 6.8 Hz, 2H, -CH₂-); 3.09 (s, 6H, -CH₃); 1.90 (m, 4H, -CH₂-); 1.54 (m, 4H, -CH₂-). ¹³C NMR (100 MHz, δ, ppm, CDCl₃): 164.79, 164.57, 159.03, 147.19, 133.23, 131.49, 131.20, 130.14, 129.56, 129.22, 127.83, 127.61, 126.67, 122.99, 121.05, 115.21, 113.97, 113.92, 113.89, 67.93, 41.75, 33.91, 32.74, 29.11, 27.97, 25.36. Mass Spectrometry (MS) (m/z) [M]⁺ Calcd for C₃₂H₃₁BrN₂O₃, 570.15; found 570.67 [M]⁺.

Synthesis of polymers



Scheme S4. The synthetic route of polymers.

The copolymers Azo(x)-Mt(y) with different copolymerization ratios were successfully synthesized by free radical polymerization. For all copolymers, x and y are the relative molar contents of the two monomers, and $x+y=1$. In this article, we only use the synthesis of Azo(0.75)-Mt(0.25) as an example to describe the synthesis process of copolymers. The copolymer Azo(0.75)-Mt(0.25) was synthesized by free radical polymerization method using AIBN as the initiator and refined THF as the solvent. The procedure of operation is described as follows: 191.1 mg MA6Azo1C, 37.3 mg MC0Mt, 1.1 mg AIBN and 533 mL refined THF were sequentially added into a clean polymerization tube. The polymerization tube was then frozen with liquid nitrogen, vacuumed and deoxygenated with an oil pump for 5 min. After that, the tube was thawed in methanol, and then N_2 was blown into the polymerization tube. The above operations were repeated for four times, and then the tube was sealed. The sealed polymerization tube was placed in an oil bath and reacted at 75°C for 7 hours. After that, the glass polymerization tube was opened and the reactant was slowly added into 250 mL mixed solvent ($V_{\text{methylene chloride}}: V_{\text{petroleum ether}} = 1:3$) by disposable syringe. The unpolymerized monomers were well dissolved in the mixed solvent, while the copolymer was precipitated. After filtration, the copolymer was collected and dried, and then 205.6 mg target copolymer Azo(0.75)-Mt(0.25) was obtained with 90% monomer conversion. All other copolymers were also synthesized according to this method.

Preparation of liquid crystal films

A pristine quartz substrate was placed on a temperature-controlled heated stage, and a sample weighing 15-50 mg was deposited onto the quartz surface. The temperature was gradually increased to melt the sample. Subsequently, polytetrafluoroethylene films with specified thicknesses (30, 100, 150, 200 μm) were applied to both ends of the quartz substrate respectively. Another layer of quartz substrate was then overlaid onto the polytetrafluoroethylene films, and uniform spreading was achieved by applying an external force. The edges of the double-layered quartz sheet were secured with clamps and then annealed. A series of polymer films with varying thicknesses were successfully prepared according to this method.

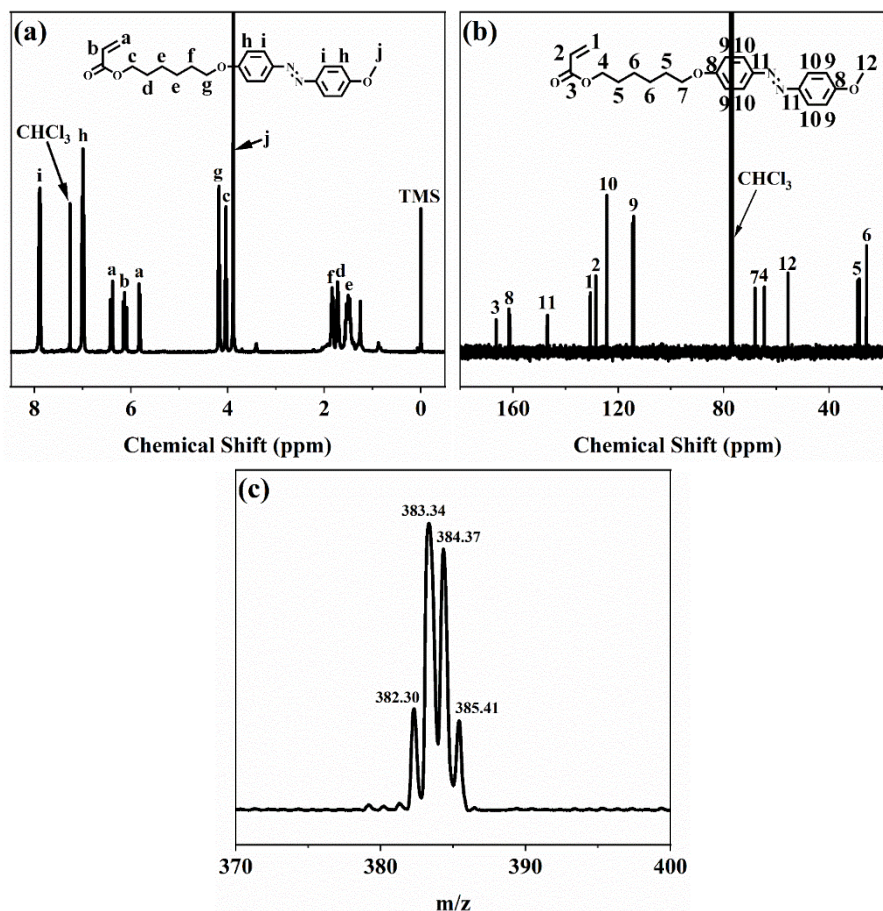


Figure S1. (a) The ¹H NMR spectrum and (b) ¹³C NMR spectrum of monomer MA6Azo1C in CDCl₃. (c) The mass spectrum of monomer MA6Azo1C in CHCl₃.

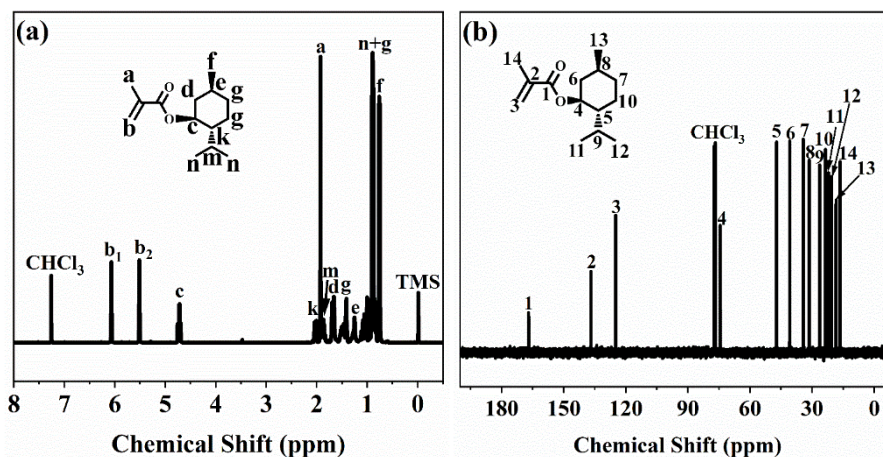


Figure S2. (a) The ¹H NMR spectrum and (b) ¹³C NMR spectrum of monomer MC0Mt in CDCl₃.

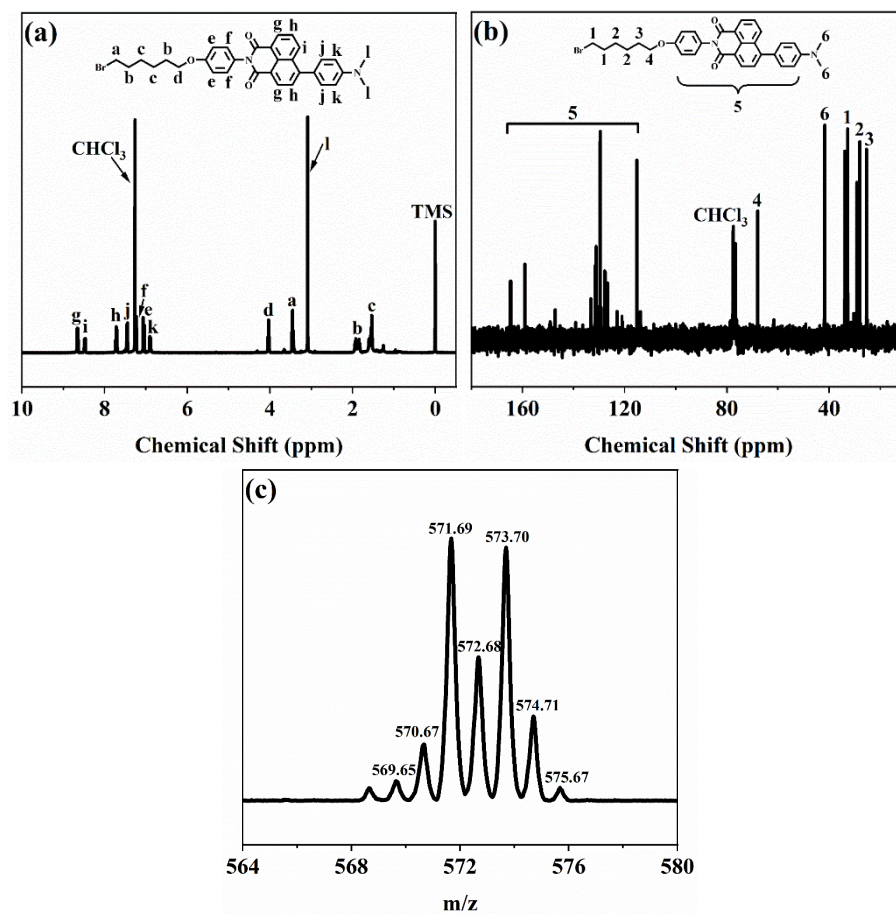


Figure S3. (a) The ¹H NMR spectrum and (b) ¹³C NMR spectrum of compound NI in CDCl₃. (c) The mass spectrum of compound NI in CHCl₃.

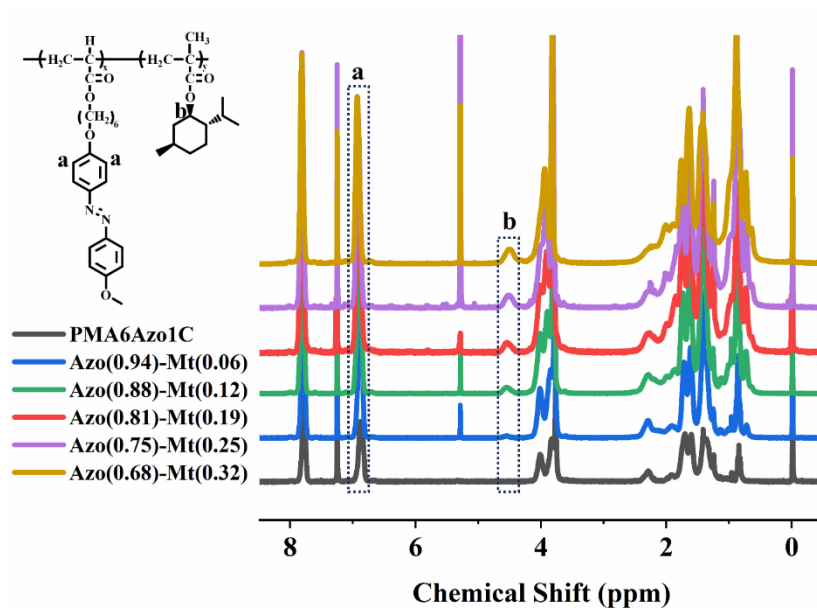


Figure S4. The ^1H NMR spectra of polymers in CDCl_3 .

Actual molar content of copolymer components

The characteristic peaks of hydrogen on the benzene ring of azobenzene (a) and the hexatomic ring of menthol (b) were chosen for calculation. The integral areas were recorded as I_a and I_b . According to Equation (SI), the actual content of azobenzene mesogens (f_{Azo}) and L-menthol groups (f_{Mt}) was calculated.

$$x = \frac{I_a}{2}, y = I_b$$

$$f_{\text{Azo}} = \frac{x}{x+y}, f_{\text{Mt}} = \frac{y}{x+y} \quad \text{Equation (SI)}$$

Table S1. GPC, TGA, and DSC test results of polymers.

Copolymers^a	M_n(×10⁴)^b	PDI^b	T_i(°C)^c	T_d(°C)^d
PMA6Azo1C	1.52	1.49	145	331
Azo(0.94)-Mt(0.06)	1.53	1.47	126	323
Azo(0.88)-Mt(0.12)	1.43	1.41	106	313
Azo(0.81)-Mt(0.19)	1.40	1.26	86	305
Azo(0.75)-Mt(0.25)	1.85	1.31	67	272
Azo(0.68)-Mt(0.32)	2.07	1.42	-	262

^a Actual mole ratio was calculated via ¹H NMR. ^b Measured by the GPC. ^c Measured by the DSC. ^d Measured by the TGA.

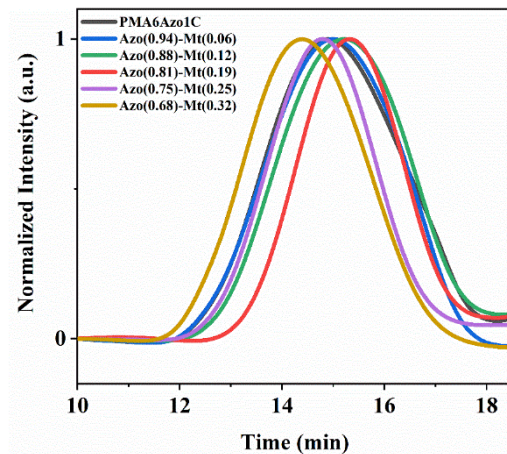


Figure S5. The GPC curves of polymers.

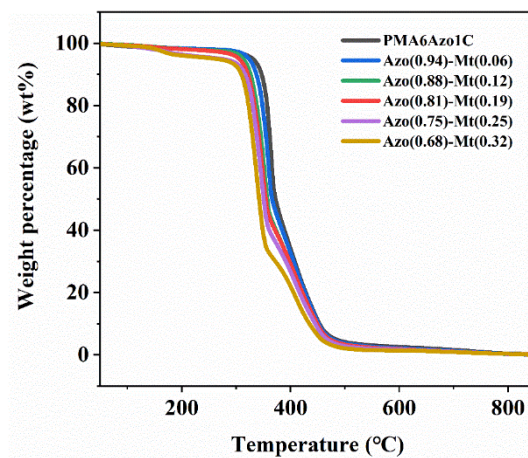


Figure S6. Thermal decomposition curves of polymers.

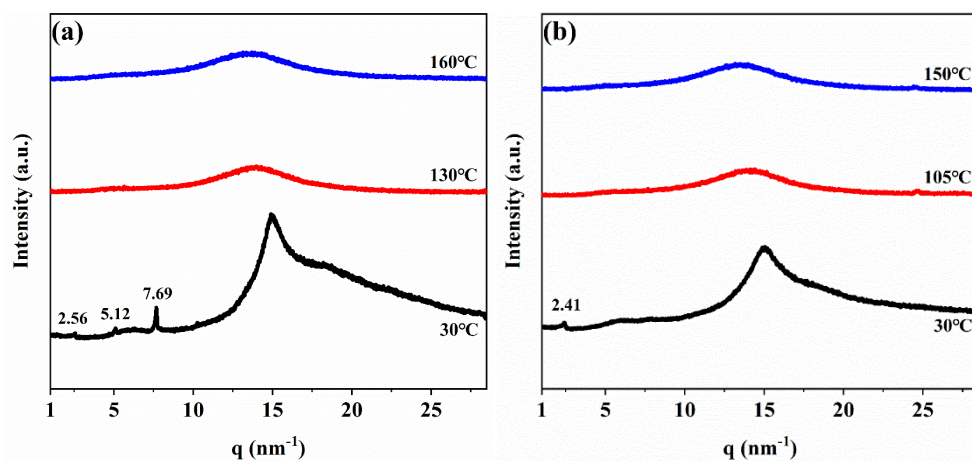


Figure S7. SAXS curves of copolymers (a) PMA6Azo1C and (b) Azo(0.94)-Mt(0.06) recorded at different temperature.

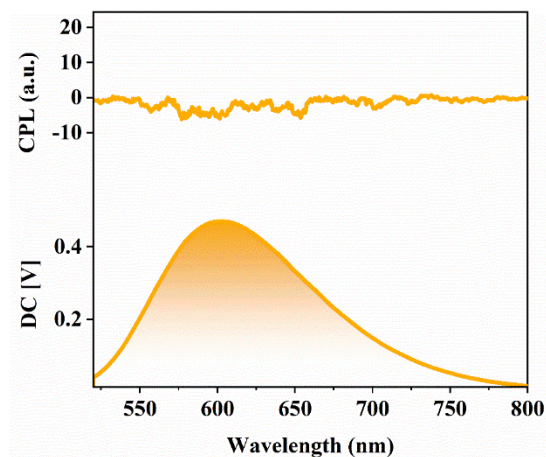


Figure S8. The CPL and DC spectra of compound NI (Temperature: 25°C, film thickness=150 μm , λ_{ex} =430 nm).

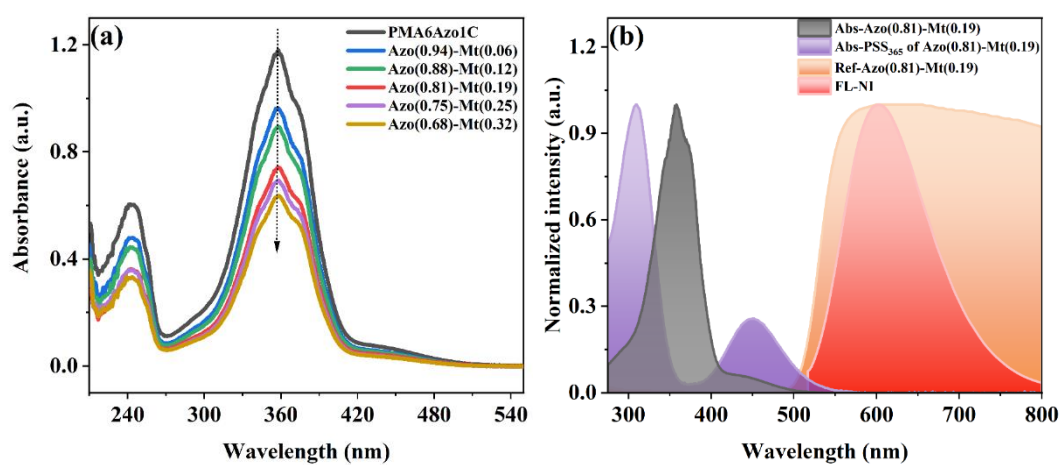


Figure S9. (a) UV-vis absorption spectra of polymer films Azo(x)-Mt(y). (b) UV-vis absorption and reflection spectra of copolymer film Azo(0.81)-Mt(0.19), and fluorescent luminescence spectrum of film NI (λ_{ex} =430 nm).

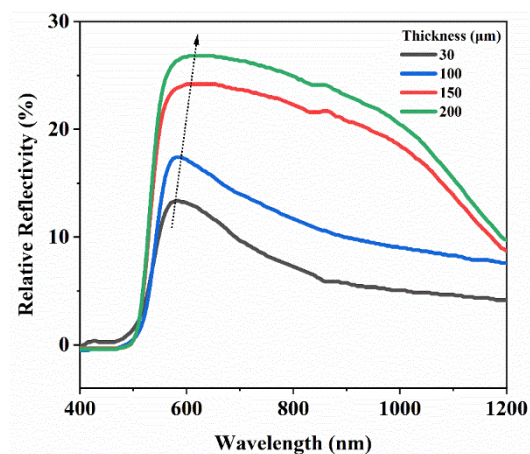


Figure S10. Reflectance spectra of copolymer Azo(0.81)-Mt(0.19) with different film thicknesses.

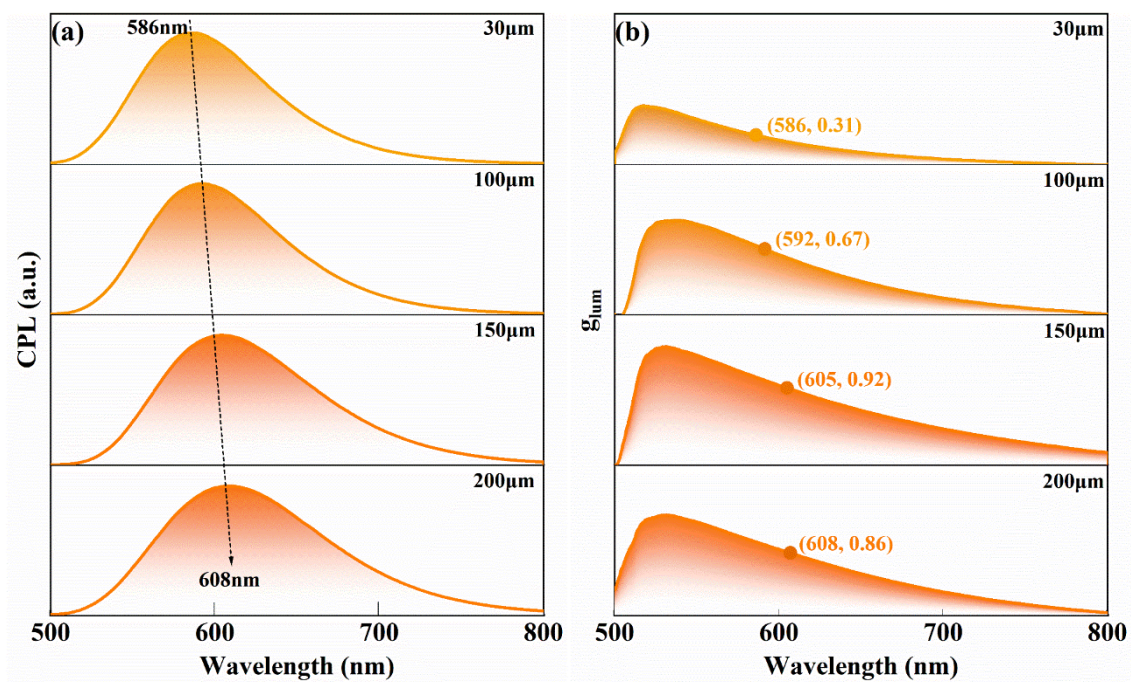


Figure S11. (a) The CPL spectra and (b) corresponding g_{lum} value spectra of copolymer NI/Azo(0.81)-Mt(0.19) with different film thicknesses (Temperature: 25°C, λ_{ex} =430 nm).

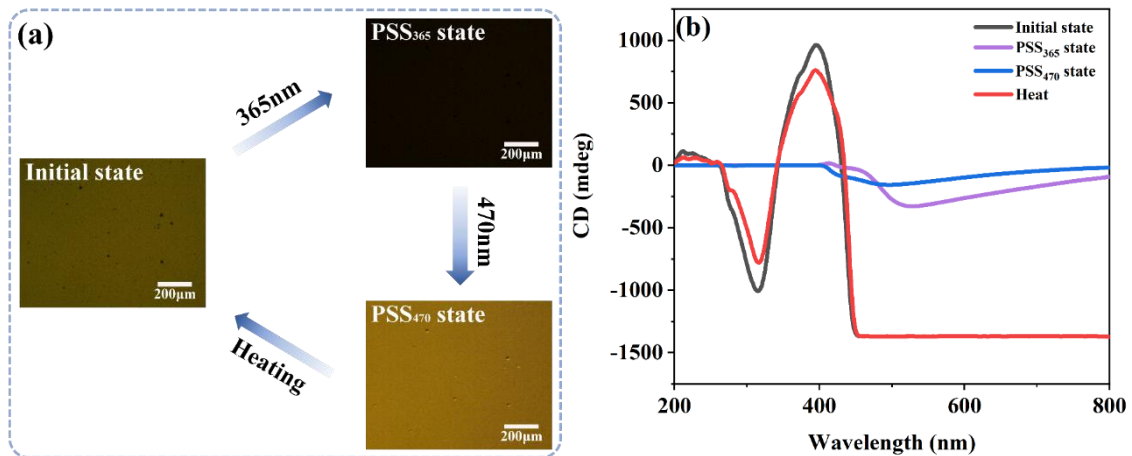


Figure S12. Photo-thermal responsive POM images (a) and circular dichroism spectra (b) of copolymer Azo(0.81)-Mt(0.19) at 25°C (Magnification: $\times 200$, film thickness=150 μm).

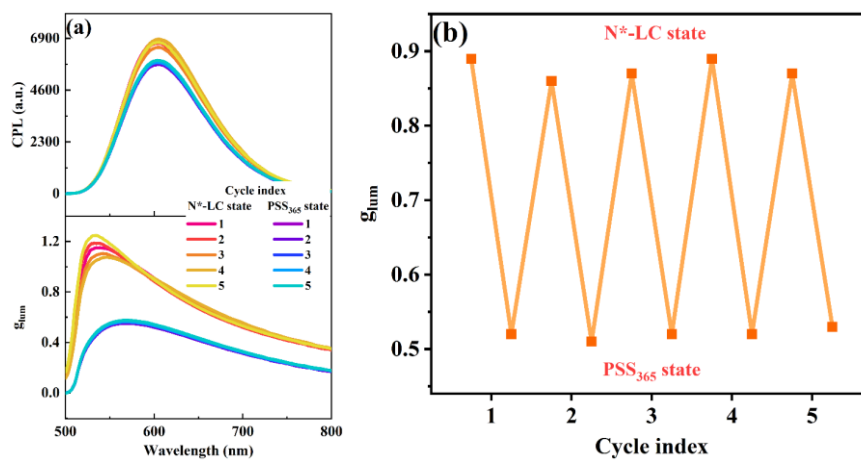


Figure S13. (a) The CPL spectra and corresponding g_{lum} value curves of the double-layered film NI/Azo(0.81)-Mt(0.19) at N*-LC state and PSS₃₆₅ state after different cycle index. (b) Variation of g_{lum} values with the cycle index. (Temperature: 25°C, film thickness=150 μm , λ_{ex} =430 nm)

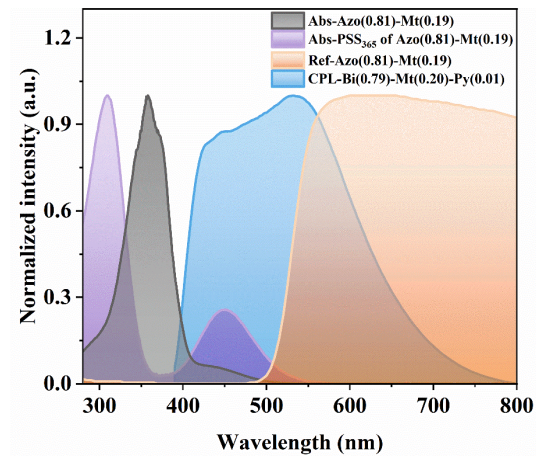


Figure S14. UV-vis absorption and reflection spectra of polymer film Azo(0.81)-Mt(0.19), and CPL spectrum of polymer film Bi(0.79)-Mt(0.20)-Py(0.01) ($\lambda_{\text{ex}}=339$ nm).